J Solid State Electrochem (2010) 14:1089–1100
DOI 10.1007/s10008-009-0918-y

ORIGINAL PAPER

Effect of thermal annealing of poly(3-octylthiophene) films covered stainless steel on corrosion properties

U. León-Silva · M. E. Nicho · J. G. González-Rodríguez · J. G. Chacón-Nava · V. M. Salinas-Bravo

Received: 26 June 2009 / Accepted: 4 August 2009 / Published online: 28 August 2009

Abstract The effect of thermal annealing of poly(3-octylthiophene) (P3OT) coatings on the corrosion inhibition of stainless steel in an NaCl solution was investigated. P3OT was synthesized by direct oxidation of the 3-octylthiophene monomer with ferric chloride ($FeCl_3$) as oxidant. P3OT films were deposited by drop-casting technique onto 304 stainless steel electrode (304SS). 304SS coated with P3OT films were thermally annealed during 30 h at different temperatures (55°C, 80°C, and 100° C). The corrosion resistance of stainless steel coated with P3OT in 0.5 M NaCl aqueous solution at room temperature was investigated by using potentiodynamic polarization curves, linear polarization resistance, and electrochemical impedance spectroscopy. The results indicated that the thermal treatment at 80°C and 100°C of P3OT films improved the corrosion resistance of the stainless steel in NaCl solution; the speed of corrosion diminished in an order of magnitude with regard to the 304SS. In order to study the temperature effect in the morphology of the coatings before and after the corrosive environment and correlate it with corrosion protection, atomic force microscopy and scanning electron microscopy were used. Morphological study showed that when the films are heated, the grain size increased and a denser surface was obtained, which benefited the barrier properties of the film.

Keywords Corrosion · Poly(3-octylthiophene) · Thermal annealed · Polymeric coatings · Stainless steel

M. E. Nicho (✉) · J. G. González-Rodríguez
Centro de Investigación en Ingeniería y Ciencias Aplicadas, UAEMor.,
Av. Universidad 1001, Col. Chamilpa,
Cuernavaca 62209 Morelos, Mexico
e-mail: menicho@uaem.mx

U. León-Silva · J. G. Chacón-Nava
Centro de Investigación en Materiales Avanzados,
Miguel de Cervantes 120, Complejo Industrial Chihuahua,
Chihuahua, Mexico

V. M. Salinas-Bravo
Instituto de Investigaciones Eléctricas,
Av. Reforma # 113,
Temixco C.P. 62490 Morelos, Mexico

Introduction

Iron and the most common iron alloy, steel, are, from a corrosion viewpoint, relatively poor materials since they rust in air, corrode in acids, and scale in furnace atmospheres. In spite of this, there is a group of iron-base alloys, the iron-chromium-nickel alloys known as stainless steels, which do not rust in sea water, are resistant to concentrated acids, and which do not scale at temperatures up to 1,100°C [1]. Nowadays, there are more than 190 different kinds of alloys that can be recognized as belonging to the stainless steel family [2]. For example, 304 stainless steels (304SSs) are extensively utilized in line pipes for chemical, petrochemical, and nuclear power industries [3]. In general, stainless steels have technological and economic importance and are used

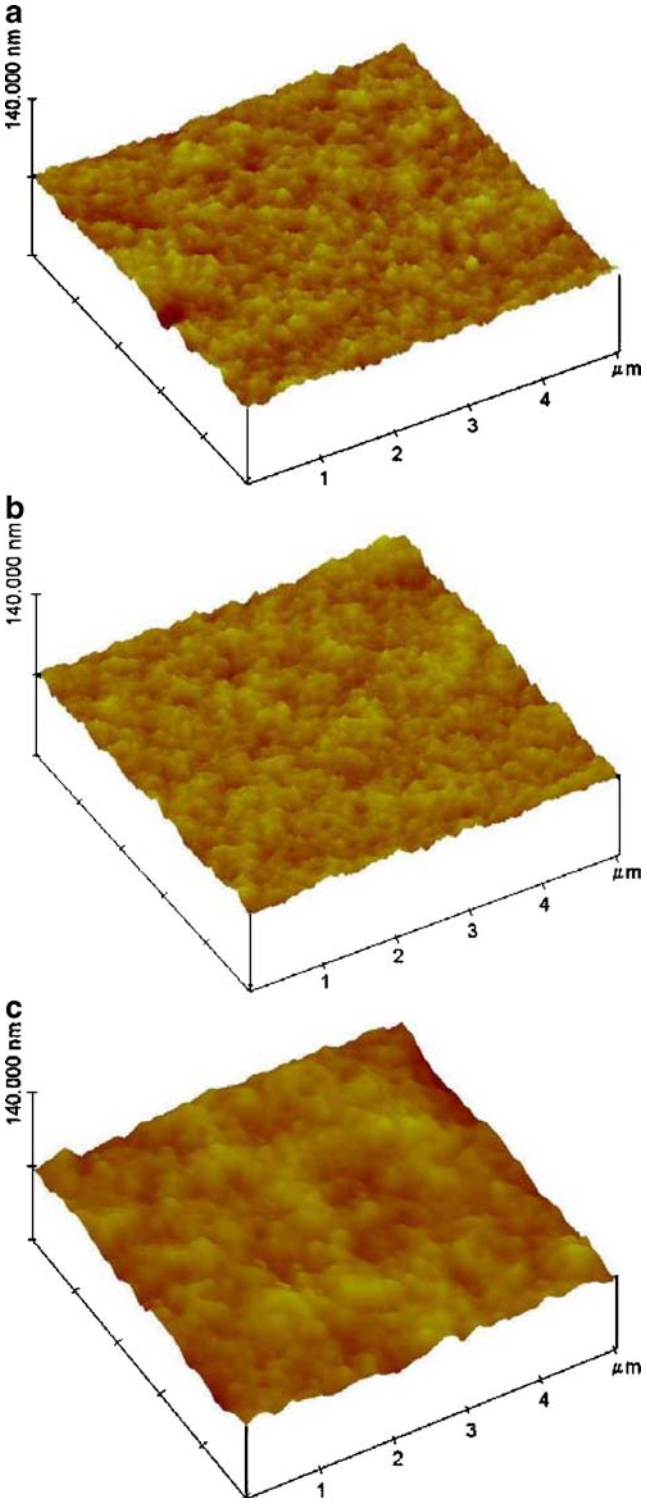

Fig. 1 Atomic force microscopy micrographs of 304SS substrates coated with P3OT annealed at (**a**) 55°C with roughness in rough media square (RMS) of 2.124 nm, (**b**) 80°C with roughness in RMS of 2.238 nm, and (**c**) 100°C with roughness in RMS of 3.515 nm

in a wide variety of services in which primary considerations are long service life (in a given environmental condition), reliability, appearance, and sanitary factors. Recent interest is the use of these materials in the medical field. Moreover, the corrosion rate of "reactive" metals and alloys can be suppressed to a great extent by modification of the metal surface by organic molecules or polymers [2]. In recent years, a considerable attention has been paid to conducting polymers due to their unique combination of properties like chemical stability, electrical conductivity, good catalytic properties, and optical and magnetic properties [4]. The mechanisms postulated by which a conducting polymer may lower the rate corrosion include the formation of a protective barrier layer, inhibition by the adsorption of organic species, and the anodic passivation achieved when the corrosion potential is shifted to more positive values under the influence of charge transfer from the conducting polymers [5]. The first reports on the corrosion protection of metals by conducting polymers were presented by Mengoli et al. and DeBerry, who studied the behavior of polyaniline (PANI) electrodeposited on steel [6, 7]. Since then, a large number of studies with focus mainly on polypyrrole (PPy) [8–11], PANI [12–17], and polythiophene were performed. Recently, electropolymerization of thiophene and its derivatives have attracted much attention, and uniform polymer films can be produced on noble metal surfaces with striking electrical properties and stability compared to other conducting polymers [18]. However, there have been few studies

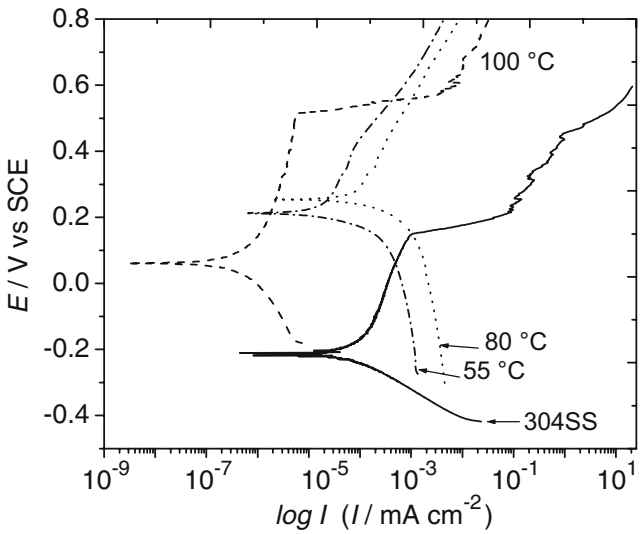

Fig. 2 Effect of annealing temperature on the polarization curves for 304SS uncoated and coated with P3OT in 0.5 M NaCl aqueous solution

Table 1 Electrochemical parameters obtained from polarization curves

Substrates	I_{corr} (mAcm^{-2})	E_{corr} (mV)	E_{pit} (mV)	E_{rup} (mV)
Uncoated 304SS	4.0 10^{-5}	−213	150	–
304SS/P3OT, 55°C	0.5 10^{-5}	210	–	491
304SS/P3OT, 80°C	5.4 10^{-5}	257	–	461
304SS/P3OT, 100°C	1.0 10^{-7}	63	–	511

about the electropolymerization of thiophene on oxidizable metals such as iron and stainless steel [19–22], due to the difficulties with polythiophene being more serious than those with PPy, since thiophene is oxidized at a much more positive potential than pyrrole (thiophene 1.8 V (vs saturated calomel electrode (SCE)) and pyrrole 0.7 V (vs SCE)) [23]. Nevertheless, Kousik et al. [20] reported that the electropolymerization of thiophene on mild steel can be achieved in acetonitrile. It was also found that electrochemically deposited polythiophene coatings have been an option to provide corrosion protection of mild steel surface in 3.5% aqueous NaCl solution. However, Rammelt et al. showed that the electrodeposition of poly (3-methylthiophene) films onto mild steel reduce the corrosion rate of mild steel, but they cannot passivate the metal surface in 0.1 M NaCl solution [23]. Tüken et al. [21] reached the synthesis of a polythiophene film on PPy-coated mild steel electrode. Galal et al. [24] and Bouklah et al. [25] showed the efficiency of some thiophene derivatives as inhibitors for the corrosion of steel.

The purpose of this study is to elucidate the effect of thermal annealed on the corrosion behavior of stainless steel coated with poly(3-octylthiophene) (P3OT) films in 0.5 M NaCl solution. Considering the difficulties with the electro-synthesis of polythiophenes and due to the cost for electrodepositing of P3OT onto 304 type stainless steel, in the present work, P3OT films were deposited by drop-casting technique onto stainless steel.

The thermal annealing was made in order to improve the physical properties of the P3OT films. In relation at this, Singh et al. have studied the correlation between changes in physical properties induced by changes in surface morphology by soft-thermal annealing in P3OT. Effect of excess heating on surface morphology and consequent changes in its physical properties reveal that annealing beyond 100°C is unsafe [26, 27]. Based on this, in the present work, the P3OT films deposited onto stainless steel were annealed at three different temperatures (55°C, 80°C, and 100°C). The corrosion protection properties before and after treatment in NaCl aqueous medium and the morphological changes in the films were studied. Until now, there has been no reports about the effect of thermal annealing in the corrosion performance of chemically polymerized soluble P3ATs in undoped/unoxidized state deposited on stainless steel in NaCl corrosive environments.

Experimental procedure

3-octylthiophene (3OT) (Aldrich) was used for the preparation of the polymeric coatings. Ferric chloride ($FeCl_3$, 98%; Aldrich), methanol (CH_3OH; Fermont), chloroform ($CHCl_3$; Baker), toluene ($C_6H_5CH_3$; Aldrich), sodium chloride NaCl (Aldrich), hydrochloric acid (HCl; Baker), and acetone ($(CH_3)_2CO$; Baker) were used as received. Commercial AISI 304 type stainless steel (304SS) sheets with 1 cm^2 in area were used as metal electrodes in this study. A copper wire of 10 cm was welded to the steel sheet with a thermocouple attachment unit equipment. Specimens with an exposure area of 10×10 mm were encapsulated with resin (MG 40 Crystal). Pre-treatment of the stainless steel substrates was carried out by polishing with different grades of emery papers down to a mirror finishing (1.0 μ alumina). They were washed

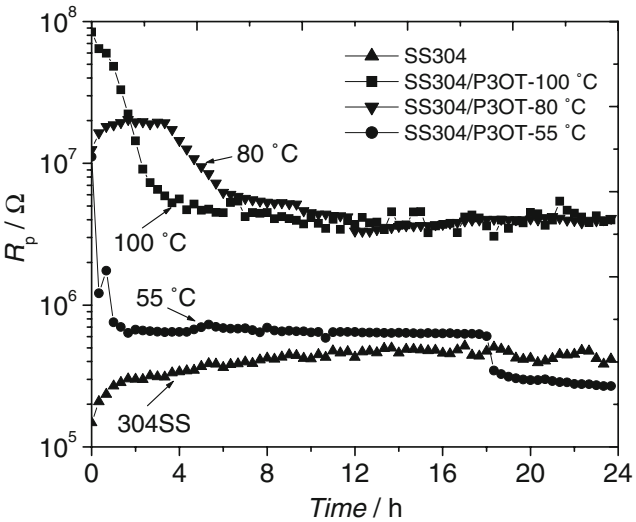

Fig. 3 Effect of annealing temperature on the change of R_p with time for 304SS uncoated and coated with P3OT in 0.5 M NaCl solution

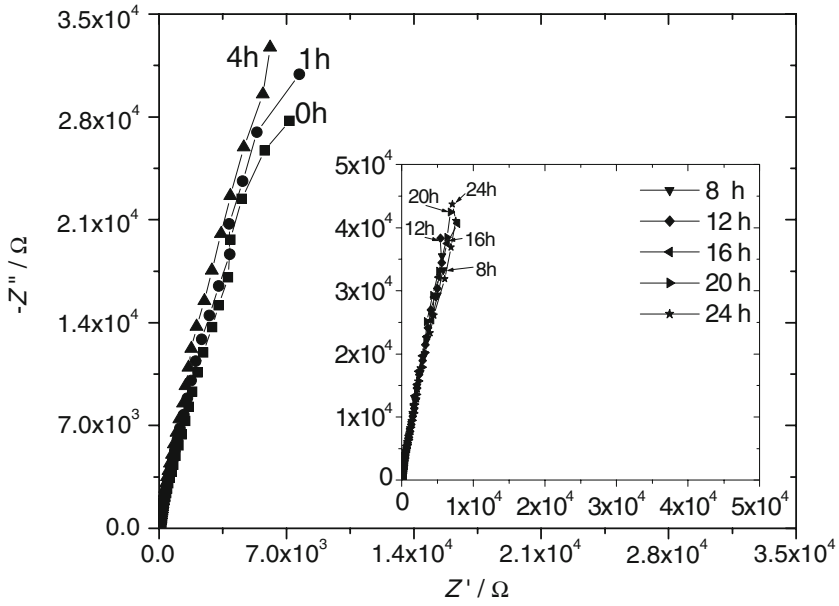

Fig. 4 Nyquist diagrams for bare 304SS at different exposure times in 0.5 M NaCl solution

with neutral soap and distilled water, degreased with ethyl alcohol, and dried with warm air before the polymeric film coating process.

P3OT polymer was synthesized by chemical oxidative polymerization technique using $FeCl_3$ as an oxidant and 3OT monomer in chloroform ($CHCl_3$) at room temperature in an inert atmosphere [28]. Anhydrous $FeCl_3$ (0.03835 mol) dissolved in $CHCl_3$ was slowly added to 0.0254 mol of 3OT dissolved in $CHCl_3$. The reaction mixture was stirred at room temperature during 25 h. The product was precipitated in methanol, filtered with a Buchner funnel, and washed three times with methanol, hydrochloric acid (10 vol.%), distilled water, and acetone. The precipitate was extracted with chloroform to isolate the chloroform-soluble fractions. The color of the soluble part was red (pristine polymer). Finally, the P3OT product was dried at 55°C.

P3OT coatings were deposited onto stainless steel sheets by drop-casting technique. This technique consists of depositing certain amount of polymeric solution (P3OT in toluene) on the electrode, and when the dissolvent is evaporated, the coating was obtained. The polymeric solution was dried within a chamber in a saturated atmosphere of toluene. After the deposition process, the coatings were annealed in static air during 30 h at three different temperatures: 55°C, 80°C, and 100°C.

Electrochemical experiments were carried out in 0.5 M NaCl aqueous solution using a standard three-electrode cell with a coated or uncoated 304SS sheet as working electrode, an SCE as reference electrode, and a graphite rod as counter electrode; the tests were performed at room temperature and controlled by an Gill AC serial number 1340 automatized potentiostat. Polarization curves were conducted over the range from −400 to 800 mV with respect to the free corrosion potential, E_{corr}, at a scan rate of 1 mV s^{-1}. Linear polarization resistance (LPR) curves were obtained by sweeping the potential region between −10 and +10 mV with respect to the free corrosion potential, E_{corr}, at

Table 2 Parameters used to simulate electrochemical impedance spectroscopy data for uncoated 304SS in 0.5 M NaCl

Element	0h	1h	4h	8h	12h	16h	20h	24h
R_s Ω	8.5	8.5	8.6	8.5	8.4	8.6	8.7	8.5
$CPE_{dl} \sim Y_o(\Omega^{-1}s^n)$	$4.7\ 10^{-5}$	$4.3\ 10^{-5}$	$4.1\ 10^{-5}$	$3.7\ 10^{-5}$	$3.4\ 10^{-5}$	$3.2\ 10^{-5}$	$3.2\ 10^{-5}$	$3.1\ 10^{-5}$
CPE_{dl} n	0.921	0.93	0.94	0.94	0.94	0.94	0.94	0.94
R_p k Ω	195.2	218.1	274.7	350.9	408.3	392.7	428.2	373.5

a scan rate of 1 mV s^{-1}, every 20 min during 24 h. Electrochemical impedance spectroscopy (EIS) tests were carried out at E_{corr} by using AC potential amplitude of 10 mV, a frequency interval of 0.1 Hz to 30 kHz during 24 h, and 100 readings per decade.

The morphology of the polymeric coatings was examined before and after corrosion tests with a Carl Zeiss DSM 960 series 6594 scanning electron microscope (SEM) and a Nano Scope IV atomic force microscope (AFM, tapping mode) with a silicone nitride tip.

Adhesion test and thickness measurement were carried out. The annealed coatings were cut in grid form. After this, a sticky tape was applied on the cut zone, and it was pressed with a pencil eraser. The tape was taken off quickly, taking the free end and raising it. The cut area was reviewed, and the loosening of the coating was evaluated. For the experimental procedure and analysis of results, the ASTM 3359 norm was consulted.

The thickness of the coatings was measured with a digital micrometer, mark Mitutoyo. Three measurements were carried out for both bare and coated steel. The average value was determined in each case. Finally, the bare steel average thickness was subtracted of polymer coated steel average thickness.

Results and discussion

Figure 1 shows AFM micrographs of the as-deposited P3OT films onto stainless steel annealed at 55°C, 80°C, and

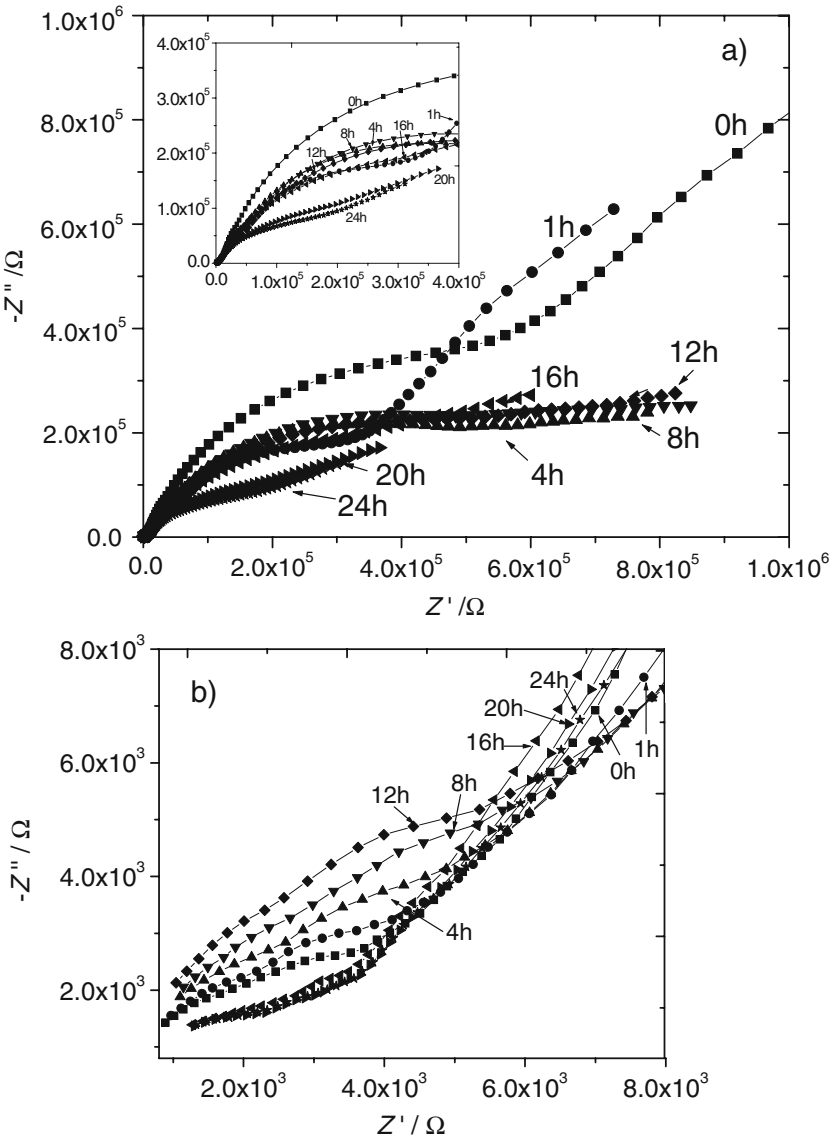

Fig. 5 Nyquist diagrams for 304SS coated with P3OT annealed at 55°C at different exposure times in 0.5 M NaCl solution (**a**) and (**b**) different amplifications

100°C. The results showed in all cases a granular homogeneous morphology. It can be seen that by increasing the annealing temperature of the P3OT coatings, coarser grain and higher roughness of the surface were obtained. Also, by increasing the annealing temperature, the films showed grains coalescence. In the case of the P3OT coating annealed at 100°C (Fig. 1c), a denser and smoother surface was observed.

According to ASTM 3359 norm, the adherence is measured as 0B, 1B, 2B, 3B, and 4B, where 0B correspond to coating with the weaker adherence and 4B to the higher adherence. The polymeric coatings annealed at 55°C and 80°C showed a good adherence, between 2B and 3B, and the coating annealed at 100°C showed a higher adherence, between 3B and 4B. The better adherence showed by the polymeric coating annealed at 100°C was due to the polymer being highly softened, and the physic interaction in the coating/metal interface was improved.

On the other hand, the temperature did not affect the coatings thickness; it was probably because the same solution quantity was used, and the polymer did not melt. The thickness of the coatings was 12 μm for coatings annealed at 55°C and 100°C, and 11 μm for coating annealed at 80°C.

Figure 2 shows the effect of annealing temperature on the polarization curves for 304SS uncoated and coated with P3OT after 1 h of exposure to 0.5 M NaCl solution. Electrochemical parameters such as corrosion current density (I_{corr}), corrosion potential (E_{corr}), pitting potential (E_{pit}), and rupture potential (E_{rup}) are given in Table 1. The lowest I_{corr} value was exhibited by P3OT coatings annealed to 100°C around 1.0 10^{-7}mA cm^{-2}, two orders of magnitude lower than uncoated 304SS. However, the P3OT coatings annealed at 55°C and 80°C showed an I_{corr} value around 0.5 10^{-5} and 5.4 10^{-5}mA cm^{-2}, respectively, remaining in the same order of magnitude than uncoated 304SS (4.0 10^{-5}mA cm^{-2}). In addition, the polymeric coatings increased the E_{corr} values with respect to bare metal for at least 276 mV (for the 304SS/P3OT, 100°C), 470 mV (for the 304SS/P3OT, 80°C), and 423 mV (for the 304SS/P3OT, 55°C). This indicates the corrosion protection of the P3OT coatings. The E_{corr} and I_{corr} values were calculated by Tafel extrapolation.

Figure 3 shows the change in polarization resistant (R_p) with time in 0.5 M NaCl solution for uncoated 304SS and coated with P3OT annealed at different temperatures. The P3OT-coated 304SS annealed at 100°C showed the highest R_p value, namely the lowest corrosion rate, at the beginning of the test up to almost three orders of magnitude higher than uncoated 304SS. It can be seen that the R_p value decreased with the time, and after 3 h, a

Table 3 Parameters used to simulate electrochemical impedance spectroscopy data for P3OT coated 304SS annealed at 55°C in 0.5 M NaCl

Element		0h	1h	4h	8h	12h	16h	20h	24h
R_s Ω		890	950	1,050	1,150	1,050	1,200	1,250	1,300
CPE_{coat} $^{\sim}Y_o(\Omega^{-1}s^n)$		3.8 10^{-7}	2.8 10^{-7}	2.8 10^{-7}	2.2 10^{-7}	6.5 10^{-8}	1.2 10^{-6}	3.8 10^{-7}	5.9 10^{-7}
CPE_{coat} n		0.587	0.599	0.583	0.61	0.708	0.451	0.555	0.509
R_{coat} k Ω		11.6	14.1	19.6	25	19.4	10.8	7.1	8.1
CPE_{dl} $^{\sim}Y_o(\Omega^{-1}s^n)$		2.1 10^{-7}	2.4 10^{-7}	2.1 10^{-7}	2.1 10^{-7}	2.3 10^{-7}	4.3 10^{-7}	6.4 10^{-7}	6.5 10^{-7}
CPE_{dl} n		0.783	0.742	0.73	0.703	0.679	0.699	0.657	0.653
R_p k Ω		1,000	540.9	694.4	790.1	760.6	585.4	305.7	251.9
W	R_w	2.2 10^6	1.9 10^6	2.8 10^6	2.1 10^6	3.4 10^6	3.2 10^6	1.6 10^6	8.0 10^5
	s	5.73	7.61	337	21	1,047	1,048	283.5	45.5
	α	0.338	0.507	0.127	0.166	0.126	0.176	0.235	0.175

steady state value was reached, and the R_p value was one order of magnitude higher than uncoated 304SS. For the P3OT-coated 304SS annealed at 80°C and 55°C, at the beginning of the test, the R_p value was about 1.0 $10^7\Omega$, almost two orders of magnitude higher than bare 304SS. In the first case, the steady state was reached after 6 h, and the R_p value was one order of magnitude higher than bare 304SS. In the case of the P3OT-coated 304SS annealed at 55°C, after the steady state was reached, the R_p values were similar to those shown by bare 304SS. The decline of R_p is due to the amount of water in the pores of the coating increases and, therefore, the mobility of the corrosive species through the coating also increases.

For corrosion protection in the immersed case, as tested here, the main positive effect (at least before breakdown) of pristine polymers is obstruct the diffusion of corrosive species. Perhaps the best corrosion performance of the films annealed at 100°C and 80°C at all times of immersion in comparison with the films annealed at 55°C is due to their diminished porous and defects. According to AFM micrographs, when the films are heated, the grain size increased, and a denser surface was obtained. It is correlated with a better barrier properties, thus, the better corrosion performance of the films annealed at 100°C and 80°C was due at their denser surface (Fig. 1b, c), through which the electrolyte had more difficulty to diffuse and reach the

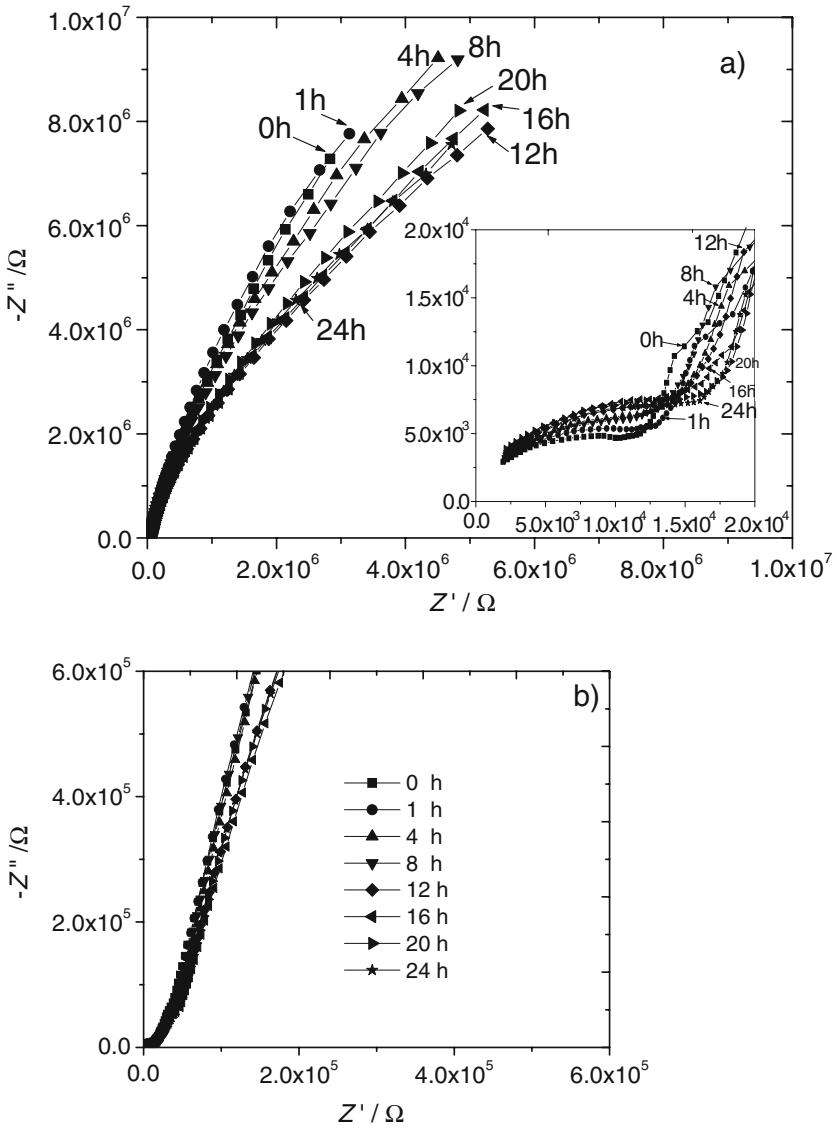

Fig. 6 Nyquist diagrams for 304SS coated with P3OT annealed at 80°C at different exposure times in 0.5 M NaCl solution (**a**) and (**b**) different amplifications

underlying metal. In this case, only barrier properties are tested here and no active role of the conducting polymer in the corrosion performance.

EIS was employed to quantify the difference in the corrosion protection obtained by the effect of thermal annealing of the P3OT-coated stainless steel in 0.5 M NaCl aqueous solution for 24 h of exposition. Figure 4 shows the Nyquist diagram for uncoated 304SS at different immersion times in 0.5 M NaCl aqueous solution. The Nyquist diagram showed a tendency to form a semicircle, the diameter is related with the polarization resistance value $\left(R_p = R_{ct} + R_s\right)$. Equivalent electric circuit to simulate EIS data for uncoated 304SS is shown in Fig. 8a, where R_s is the solution resistance, C_{dl} is the capacitance of the electrochemical layer double and R_p. According to R_p values obtained by simulation (Table 2), they increased until 20 h of exposition at the corrosion solution, because 304SS is offering good resistance against the corrosion in this environment.

Generally, an element of constant phase (CPE) is used instead of a pure capacitance (C) due to a distribution of the relaxation times as a result of inhomogeneities present on the electrode. This may result from contributions from static disorder such as porosity, random mixture of conductor and insulator that can be described by the effective medium approximation at percolation, or an interface that can be described by either a fractal geometry concept or an RC transmission line concept. The CPE can also include contribution from a dynamic disorder such as diffusion. The impedance of a constant phase element is defined as:

$$Z_{CPE} = [Q(jw)^n]^{-1} \text{with} -1 \leq n \leq 1$$

where Z (Ohms cm^2) is the electrode impedance. The constant Q (Ohms^{-1} s^n cm^{-2}) is a combination of properties related to both the surface and the electroactive species and is independent of frequency. The exponent n is related to a slope of the log Z against log f Bode plot, i.e., to the phase angle θ by the relation $n = 2\theta/\pi$ and $j = (-1)^{0.5}$. A pure capacitance yields $n = 1$, a pure resistance yields $n = 0$, and a pure inductance yields $n = -1$, while $n = 0.5$ represents the Warburg impedance [29].

Figure 5 shows the Nyquist diagram of 304SS coated with P3OT annealed at 55°C and immersed in 0.5 M NaCl. Two semicircles partially formed were observed, the high frequencies semicircle represents the impedance response of the P3OT coating, while the medium frequencies semicircle is attributed to the charge transfer resistance (R_{ct}). Also, a right line approximately at 45°

Table 4 Parameters used to simulate electrochemical impedance spectroscopy data for P3OT coated 304SS annealed at 80°C in 0.5 M NaCl

Element		0h	1h	4h	8h	12h	16h	20h	24h
R_s Ω		202.5	180	181.5	200	182.5	180.8	161.3	212.6
CPE_{coat} $^{\sim}Y_o(\Omega^{-1}s^n)$		$2.1\ 10^{-8}$	$2.2\ 10^{-8}$	$2.3\ 10^{-8}$	$2.7\ 10^{-8}$	$2.4\ 10^{-8}$	$2.1\ 10^{-8}$	$1.9\ 10^{-8}$	$1.9\ 10^{-8}$
CPE_{coat} n		0.777	0.763	0.761	0.744	0.751	0.758	0.759	0.765
R_{coat} k Ω		13.8	15.6	18.1	17.1	20.2	21.4	21.5	20.3
W	R_w	37,077	72,228	99,047	97,698	91,109	98,143	98,804	79,889
	s	0.002	0.006	0.006	0.006	0.004	0.004	0.005	0.004
	α	0.424	0.437	0.441	0.447	0.436	0.431	0.43	0.428
CPE_{dl} $^{\sim}Y_o(\Omega^{-1}s^n)$		$1.6\ 10^{-7}$	$1.5\ 10^{-7}$	$1.1\ 10^{-7}$	$1.1\ 10^{-7}$	$1.1\ 10^{-7}$	$1.1\ 10^{-7}$	$1.1\ 10^{-7}$	$1.2\ 10^{-7}$
CPE_{dl} n		0.879	0.904	0.869	0.851	0.825	0.816	0.826	0.831
R_p k Ω		38,000	35,000	37,000	38,000	26,000	29,000	31,000	26,000

with respect to Z' axis was observed at low frequencies, which is attributed to diffusion processes through the P3OT coating [30, 31]. Thus, the water molecules involved in the diffusion process induce a loss of adherence in localized zones of coating/metal interface. In addition, water absorbed on the steel surface creates an electrolyte for the reduction of oxygen and the oxidation of iron [32]. According to R_{coat} values obtained by simulation (Table 3), they increased until 8 h of exposition at the corrosion solution, because the pores were blocked by the corrosion products [21]. After 8 h, the R_{coat} declines because the amount of water in the pores increases and therefore enhances the mobility of corrosive species through the coating. Because of the decline of R_{coat}, the R_p is also affected and diminishes its value (Table 3), increasing the speed of corrosion.

When the 304SS coated with P3OT was annealed at 80°C and after it was immersed in 0.5 M NaCl, Fig. 6, the Nyquist diagram, showed two depressed semicircles, one of them in high frequency and the other partially formed in medium-low frequencies. The behavior in high frequency is related to the coating, while the medium-low frequency behavior corresponds to the reactions occurring on the metal through defects and pores in the coating [30]. A line quasi-vertical followed by the semicircle related to the coating was also observed. This behavior is attributed to the diffusion (Warburg impedance) of corrosive species through the coating. After 0 h exposure, the R_{coat} increases (Table 4) because the pores of the coating are blocked by the corrosion products generated by the diffusion of the corrosive species.

In the case of the P3OT coating annealed at 100°C (Fig. 7), two overlap semicircles were observed. The semicircle in high-medium frequencies is attributed to the coating and the low frequency to the R_{ct}. In this case, an R_{coat} greater than the one obtained with the coatings annealed at 55°C and 80°C was obtained through simulation (Tables 3, 4, and 5).

The coatings annealed at 80°C and 100°C showed greater R_p, about one order of magnitude greater than the R_p obtained for the uncoated 304SS (Tables 2, 4, and 5). The P3OT-coated 304SS annealed at 55°C showed values of R_p (Table 3) very similar to those of uncoated 304SS. In the case of P3OT, 100°C did not present a diffusion mechanism.

Equivalent electric circuits to simulate EIS data for uncoated and P3OT-coated 304SS are given in Fig. 8, where CPE_{coat} and R_{coat} represent the capacitance and resistance of the coating, respectively, CPE_{dl} represent the constant phase element of the electrochemical double layer, and W represent impedance Warburg.

The results obtained in the corrosion tests were corroborated by SEM microscopy. Figure 9a–c shows the micrographs of P3OT coatings annealed to 55°C, 80°C, and 100°C, respectively, before the corro-

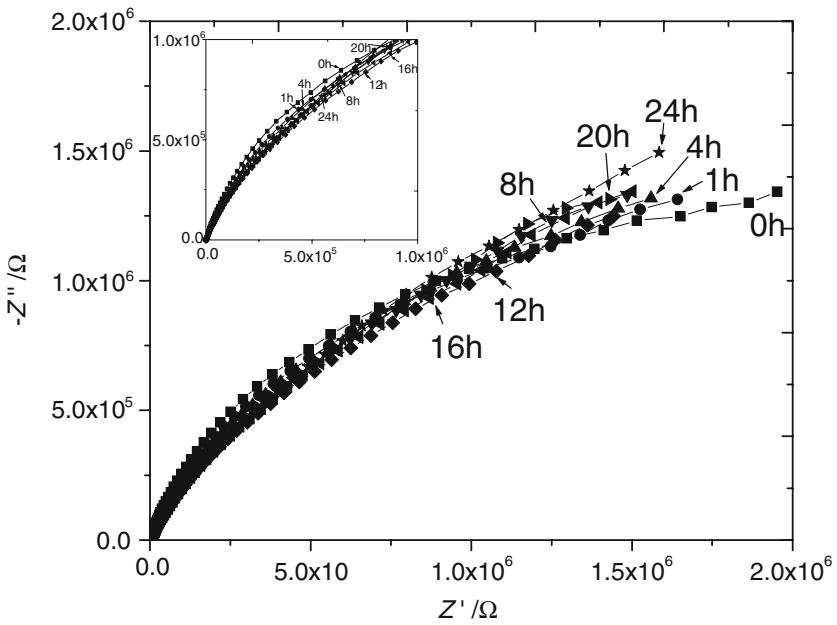

Fig. 7 Nyquist diagrams for 304SS coated with P3OT annealed at 100°C at different exposure times in 0.5 M NaCl solution

Table 5 Parameters used to simulate electrochemical impedance spectroscopy data for P3OT coated 304SS annealed at 100°C in 0.5 M NaCl

Element	0h	1h	4h	8h	12h	16h	20h	24h
R_s Ω	151	147.2	147	145.8	140.8	138.1	161	149.1
CPE_{coat} $\tilde{Y}_o(\Omega^{-1}s^n)$	$2.7\ 10^{-7}$	$3.7\ 10^{-7}$	$4.7\ 10^{-7}$	$4.2\ 10^{-7}$	$4.2\ 10^{-7}$	$4.1\ 10^{-7}$	$4.4\ 10^{-7}$	$3.7\ 10^{-7}$
CPE_{coat} n	0.807	0.781	0.761	0.751	0.74	0.735	0.755	0.753
R_{coat} k Ω	3,200	3,600	4,100	3,600	3,300	3,600	3,400	3,300
CPE_{dl} $\tilde{Y}_o(\Omega^{-1}s^n)$	$2.6\ 10^{-7}$	$3.6\ 10^{-7}$	$4.1\ 10^{-7}$	$4.6\ 10^{-7}$	$4.7\ 10^{-7}$	$4.7\ 10^{-7}$	$6.4\ 10^{-7}$	$4.4\ 10^{-7}$
CPE_{dl} n	0.464	0.45	0.551	0.513	0.579	0.53	0.657	0.606
R_p k Ω	7,500	10,000	71,000	11,000	6,700	10,000	7,700	8,000

sion test. These micrographs show a homogeneous morphology with some defects (such as pores and pinholes) in the surface. Figure 9d–f shows these coatings after they have been corroded during 24 h in NaCl. In the case of stainless steel coated by P3OT annealed at 55°C (Fig. 9d), several blisters and some holes (blown blisters) were observed almost throughout the surface. The blisters are developed because of the loss of adhesion between coating and substrate in localized areas, which allowed the dissemination of electrolyte to the coating/metal interface to subsequently corrode the material. In the case of 304SS coated with P3OT annealed at 80°C (Fig. 9e), it was observed that the coating presented only small blisters throughout the surface; however, 304SS coated with P3OT annealed at 100°C (Fig. 9f) showed no blisters. Thus, the least degraded coating was achieved at temperature 100°C. As the annealing temperature decresed, the degree of degradation was increased. With the results obtained, we could say that the coating first allows the dissemination of electrolyte toward the metal surface and, subsequently, the formation of blisters. Finally, the metal corroded.

Conclusions

The effect of thermal annealing of P3OT coatings on the corrosion inhibition of 304SS in 0.5 M NaCl solution was investigated using electrochemical methods. The 304SS under the conditions submitted in this investigation showed an anodic current limit in the polarization curves. It was observed in the polarization curves that the presence of the P3OT coatings onto 304SS increases the value of the corrosion potential and decreases corrosion current density on the values obtained for uncoated 304SS. LPR results showed that by using P3OT treated at 80°C and 100°C as coating onto 304SS, the corrosion rate was lowered by one order of magnitude higher than bare 304SS, thus these coatings showed the best protection against the corrosion of 304SS in NaCl medium. EIS results showed that Warburg type impedance was observed, indicating that the corrosion mechanism was under a mixed control: charge transfer from the metal to the environment through the double electrochemical layer, and by diffusion of aggressive ions through the polymeric coatings. Probably the better corrosion performance of the P3OT films annealed at 80°C and 100°C was due to their denser surface, through which the electrolyte had more difficulty to diffuse and reach the underlying metal. All this was corroborated by means of SEM and AFM.

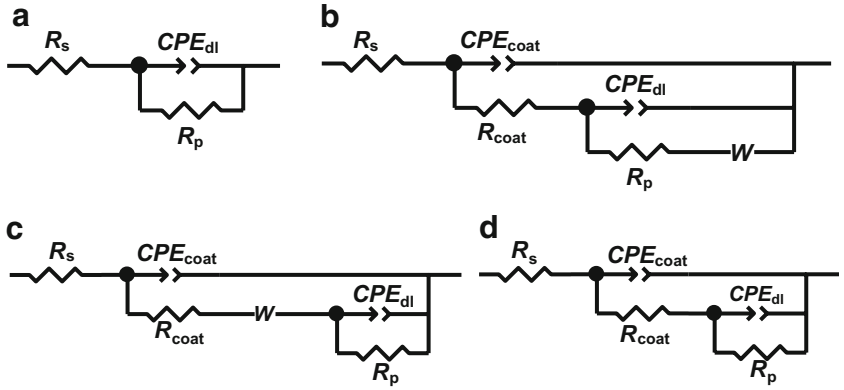

Fig. 8 Equivalent electric circuits used to simulate electrochemical impedance spectroscopy data for (**a**) uncoated 304SS and P3OT-coated 304SS annealed at (**b**) 55°C, (**c**) 80°C, and at (**d**) 100°C

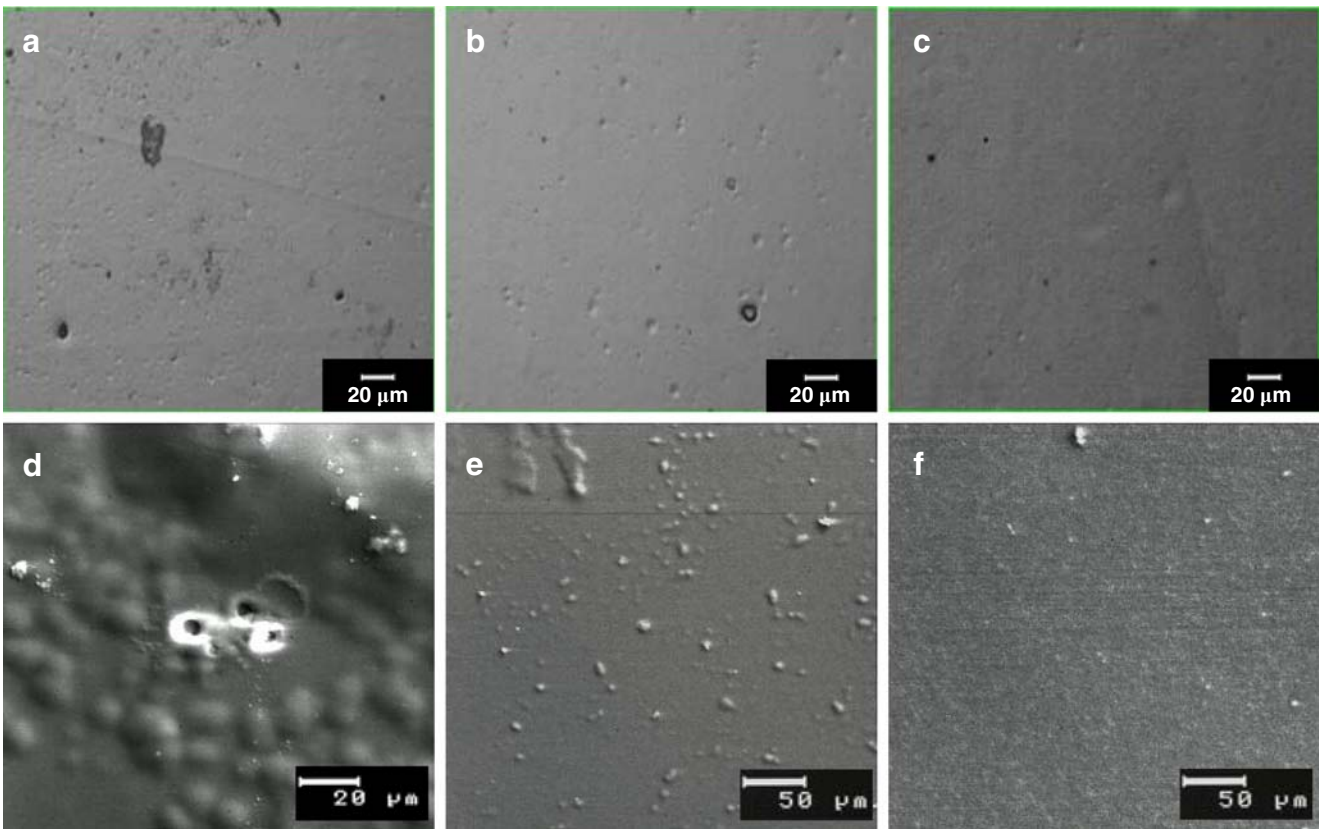

Fig. 9 Scanning electron microscopy micrographs of 304SS substrates coated with P3OT annealed at (**a**, **d**) 55°C, (**b**, **e**) 80°C, and (**c**, **f**) 100°C (**a**–**c**) before the corrosion tests and (**d**–**f**) after the corrosion tests in 0.5 M NaCl solution

Acknowledgements The authors thank the financial support from *Consejo Nacional de Ciencia y Tecnología* (CONACYT, Mexico, 52598-R) and Daniel Bahena Uribe for AFM images.

References

1. Leffler B (2001) STAINLESS—stainless steels and their properties
2. Galal A, Atta NF, Al-Hassan MHS (2005) Mater Chem Phys 89:38
3. Tsay LW, Yu SC, Huang RT (2007) Curr Sci 49:2973
4. Rokovic MK, Kvastek K, Horvat-Radosevic V, Duic LJ (2007) Curr Sci 49:2567
5. Hür E, Bereket G, Sahin Y (2006) Mater Chem Phys 100:19
6. Mengoli G, Munari MT, Bianco P, Musiani MM (1981) J Appl Polym Sci 26:4247
7. Deberry DW (1985) J Electrochem Soc 132(5):1022
8. Le HNT, Garcia B, Deslouis C, Xuan QL (2002) J Appl Electrochem 32:105
9. Akundy GS, Rajagopalan R, Iroh JO (2002) J Appl Polym Sci 83:1970
10. Tüken T (2006) Surf Coat Technol 200:4713
11. Lallemand F, Auguste D, Amato C, Hevesi L, Delhalle J, Mekhalif Z (2007) Electrochim Acta 52:4334
12. Souza S (2007) Surf Coat Technol 201:7574
13. Dominis A, Spinks G, Kane-Maguire LAP, Wallace GG (2002) Polym Prepr 41:1748
14. Kilmartin PA, Trier L, Wright GA (2002) Synth Met 131:99
15. Berry BC, Shaikh AU, Viswanathan T (2000) Polym Prepr 41:1739
16. Yeh JM, Liou SJ, Lai CY, Wu PC (2001) Chem Mater 13:1131
17. Sathiyanarayanan S, Azim SS, Venkatachari G (2007) Synth Met 157:205
18. Tüken T, Yazıcı B, Erbil M (2005) Appl Surf Sci 239:398
19. Ren S, Barkey D (1992) J Electrochem Soc 139:1021
20. Kousik G, Pitchumani S, Renganathan NG (2001) Prog Org Coat 43:286
21. Tüken T, Yazici B, Erbil M (2004) Prog Org Coat 51:205
22. Deng Z, Smyrl WH, White HW (1989) J Electrochem Soc 136:2152
23. Rammelt U, Nguyen PT, Plieth W (2001) Electrochim Acta 46:4251
24. Galal A, Atta NF, Al-Hassan MHS (2005) Mater Chem Phys 89:28
25. Bouklah M, Hammouti B, Aouniti A, Benhadda T (2004) Prog Org Coat 49:225
26. Singh R, Kumar J, Singh RK, Kaur A, Sood KN, Rastogi RC (2005) Polymer 46:9126
27. Kumar J, Singh RK, Rastogi RC, Singh R (2007) Mater Chem Phys 101:336
28. Sugimoto R, Takeda S, Gu HB, Yoshino K (1986) Chem Express 1:635
29. Omanovic S, Roscoe SG (1999) Langmuir 15:8315
30. Hang TTX, Truc TA, Nam TH, Oanh VK, Jorcin JB, Pébère N (2007) Surf Coat Technol 201:7408
31. Galicia P, Batina N, González I (2006) J Phys Chem B 110:14398
32. Han M, Hu Y, Sharma R, Warren GW, Nikles DE (2000) Polym Prepr 41:1757